

---

# ConfounderGAN: Protecting Image Data Privacy with Causal Confounder

---

Qi Tian<sup>1</sup> Kun Kuang<sup>1,5,\*</sup> Kelu Jiang<sup>1</sup> Furui Liu<sup>2</sup> Zhihua Wang<sup>3</sup> Fei Wu<sup>1,3,4,5</sup>

<sup>1</sup> College of Computer Science and Technology, Zhejiang University, Hangzhou, China

<sup>2</sup> Huawei Noah's Ark Lab, Beijing, China

<sup>3</sup> Shanghai Institute for Advanced Study of Zhejiang University, Shanghai, China

<sup>4</sup> Shanghai AI Laboratory, Shanghai, China

<sup>5</sup> Key Laboratory for Corneal Diseases Research of Zhejiang Province, Hangzhou, China  
{tianqics,kunkuang,jiangkelu,zhihua.wang,wufei}@zju.edu.cn

## Abstract

The success of deep learning is partly attributed to the availability of massive data downloaded freely from the Internet. However, it also means that users' private data may be collected by commercial organizations without consent and used to train their models. Therefore, it's important and necessary to develop a method or tool to prevent unauthorized data exploitation. In this paper, we propose *ConfounderGAN*, a generative adversarial network (GAN) that can make personal image data unlearnable to protect the data privacy of its owners. Specifically, the noise produced by the generator for each image has the confounder property. It can build spurious correlations between images and labels, so that the model cannot learn the correct mapping from images to labels in this noise-added dataset. Meanwhile, the discriminator is used to ensure that the generated noise is small and imperceptible, thereby remaining the normal utility of the encrypted image for humans. The experiments are conducted in six image classification datasets, consisting of three natural object datasets and three medical datasets. The results demonstrate that our method not only outperforms state-of-the-art methods in standard settings, but can also be applied to fast encryption scenarios. Moreover, we show a series of transferability and stability experiments to further illustrate the effectiveness and superiority of our method.

## 1 Introduction

In recent years, deep learning has achieved great success in many fields, such as computer vision [10], natural language processing [6], *etc.* An important factor is that large-scale datasets provide rich and diverse training examples for deep neural networks. However, many datasets are collected from some free channels without mutual consent, and this unauthorized collection of private data may violate the rights of the data owner [3]. For example, Kashmir Hill from the New York Times recently reported that a company, named Clearview.AI, used web crawler scripts to collect more than 3 billion online photos from various multimedia websites (*e.g.*, Facebook) for training its own commercial models [35]. This large unauthorized dataset goes far beyond anything ever constructed by the United States government or Silicon Valley giants. In addition, Google's Nightingale Project has also been reported to collect medical care information from tens of millions of patients without their knowledge, and use advanced machine learning technology to customize medical services for individual patients [23, 37].

In this context, various information privacy laws around the world have been published to describe the rights of natural persons to control who is using its data [41]. *e.g.*, General Data Protection

\*Corresponding author.

Regulation (GDPR) in the European Union [39], Electronic Communications Privacy Act (ECPA) in the U.S. [40, 38], *etc.* However, in addition to legal constraints, it's necessary to develop a protection method to actively prevent unauthorized data from being used by third parties to train commercial models. In this paper, we aim to develop an image encryption method. *i.e.*, the deep classification models cannot extract any exploitable knowledge from encrypted (or processed) images. Moreover, we hope the modification of the original data is strictly limited, thereby retaining the data quality for normal usage. *e.g.*, an unlearnable photo should be free from obvious visual defects so it can be shared with friends on social media.

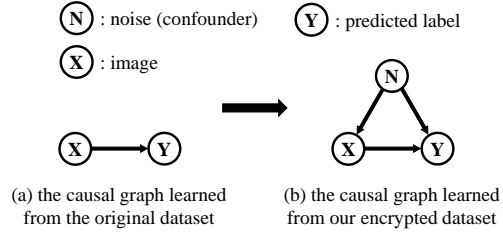


Figure 1: Causal graphs learned from the original dataset and our encrypted dataset.

Unfortunately, the existing works are very sparse and have application limitations. Shan et al. [30] first propose an error-maximizing noise based on metric learning to make data unexploitable, but this method is mainly customized for face recognition systems. Then Huang et al. [12] propose a bi-level optimization based on error-minimizing noise (EMN) to meet the above goal, and it can be extended to various image datasets. However, these methods need multiple gradient backpropagations to generate an effective noise for each labeled image, which means they cannot encrypt an unlabeled image on the fly. We emphasize that this setting is common and important for real-world applications. For example, a person takes a photo with a cell phone. Then he/she wants to quickly encrypt the photo and share it on social media immediately.

In this paper, we propose a novel image data encryption method called *ConfounderGAN* to solve the above challenges. Figure 1 demonstrates the core idea of our method. We suppose that the model can learn a correct causal graph from the image  $X$  to the label  $Y$  in the original dataset as illustrated in Figure 1(a). To prevent unauthorized models from extracting ground truth relationship  $X \rightarrow Y$  from the private dataset, we deliberately introduce a confounder noise  $N$  that satisfies the relationship  $X \leftarrow N \rightarrow Y$  in the dataset as shown in Figure 1(b). This confounder noise is correlated with both the image  $X$  and the label  $Y$ , creating a spurious correlation between  $X$  and  $Y$ . Therefore, models trained on this data would fit the negatively spurious correlation and get low test accuracy. There are many possible ways that can achieve this confounder-based encryption framework. We instantiate this framework by generative adversarial networks (GAN) [9], as this implementation is more efficient and practical. Specifically, we hope that the generator can produce confounder noise that satisfies the above causal graph for each private image. The main challenge is how to ensure that the noise is strongly associated with both the image and the label. Since the noise is produced by the generator with the original image as input, the former is naturally satisfied. For the latter, we directly classify the noise as the ground truth class of the original image during generator training. Meanwhile, we send the original image and its noise-added copy to the discriminator, thus ensuring the invisibility of noise. Once the generator is trained, it can quickly produce confounder noise for any image to protect its privacy, including those unlabeled ones. Our main contributions are:

- We present a confounder-based framework for image data encryption. The confounder in this framework can create spurious correlations between images and labels, thus preventing unauthorized models from learning exploitable knowledge on the encrypted data.
- By leveraging the property of generative adversarial networks, we implement the above framework as *ConfounderGAN*, where the generator is used to produce confounder noise to encrypt the target image and the discriminator ensures that the noise is imperceptible.
- Extensive experiments on six image classification datasets show that our proposed method not only outperforms state-of-the-art methods in standard settings, but can also be applied to fast encryption scenarios. Also, we conduct a set of transferability and stability experiments to highlight the effectiveness and superiority of our method.

## 2 Related work

In this section, we briefly review some literature that is closely related to our work: data privacy, data poisoning, causal confounder in deep learning.

**Data privacy.** Privacy-preserving techniques have been widely explored in the machine learning community and a lot of excellent works have been proposed to protect data privacy [32, 26, 27, 33]. However, these methods are mainly to prevent malicious agencies from de-inferring training set information in a trained model. In this paper, we focus on a more challenging scenario. *i.e.*, making private data completely unlearnable by unauthorized deep neural networks. Shan et al. [30] first propose a solution for the face recognition system. By utilizing the targeted adversarial attack to generate error-maximizing noise, this method can close the representation of different identities so that the model trained on this dataset can only obtain poor performance. Then Huang et al. [12] propose a bi-level optimization based on error-minimizing noise (EMN) to meet the same goal, and it is a general method that can be used to various image datasets. However, these gradient-based methods need multiple optimization steps for encrypting one labeled image, and thus cannot quickly encrypt an unlabeled one. Instead, our ConfounderGAN does not have this limitation. Because once the confounder noise generator is trained, any private image can be processed immediately.

**Data poisoning.** The goal of traditional data poisoning is to reduce the test accuracy of the model by modifying the training set. Biggio et al. [2] first introduce this type of attack in support vector machines. Then Muñoz-González et al. [21] propose a deep learning version by poisoning the most representative samples in the training examples. Although data poisoning attacks seem to share the same goal as ours, these methods have a limited impact on DNNs and are not suitable for data protection tasks. *e.g.*, the model trained on poisoned examples can still achieve acceptable performance [21], and the modified image can be easily distinguished from the original one [44]. In addition, the backdoor attack is another type of attack that poisons training data with a trigger pattern [4, 29, 20], but this attack does not prevent the model from learning useful knowledge in the natural data. Therefore, traditional data poisoning methods cannot be used for data protection, while our proposed method can produce unlearnable examples with imperceptible noise.

**Confounder in deep learning.** In statistics, a confounder is a variable that influences both the cause variable and effect variable, causing a spurious association [24]. If there are confounders in the training set, the model may be hard to learn the correct causal relationship from input to output, resulting in sub-optimal performance [17, 36]. A lot of works have been proposed to mitigate the negative impact of confounders in deep learning [31, 42, 43, 18]. *e.g.*, Shen et al. [31] believe that the background in the dataset plays the role of a confounder and they propose to improve by sample reweighting. However, all these methods treat the confounder as a defect. Instead, our proposed method utilizes the property of the confounder to achieve data privacy protection.

### 3 Problem statement

In this paper, we focus on the scenario of image data encryption. There are two characters in this scenario: data owner and unauthorized model trainer. The data owner needs to encrypt their private data to prevent the model trainer from obtaining the high-performance classification model on this data. We consider two practical encryption settings:

(1) In-distribution data encryption (standard setting)

This setting follows [30, 12]. The data owner has  $n$  labeled natural (unencrypted) data  $\mathcal{D}_{nat}$ . He/she can actively use a protection method to obtain encryption (unlearnable) images by adding imperceptible perturbation to the original images. Since the protection method has access to each data to adaptively learn and generate custom unlearnable noises, these processed data are defined as in-distribution encrypted data  $\mathcal{D}_{in,en}$ .

(2) Out-of-distribution data encryption (fast encryption setting)

The data owner trains a cryptographic tool (*e.g.*, a generator) with labeled historical data. Once the encryption tool is trained, it can be used for fast encryption on any data. Specifically, if the data owner uses this tool to encrypt the historical data (*i.e.*, the training set of the encryption tool), the processed data is denoted as  $\mathcal{D}_{in,en}$ . Instead, if they use the tool to encrypt some newly unlabeled data (*i.e.*, the non-training set of the encryption tool), the processed data is called out-of-distribution encrypted data  $\mathcal{D}_{out,en}$ . We believe this setting is practical for the real world. *e.g.*, a person can install the encryption app on the phone in advance, and then their instant photos can be quickly encrypted by this app.

One unauthorized model trainer can download any data from public sources as the training set. *i.e.*,  $\mathcal{D}_{tr} = \{\mathcal{D}_{in,en}, \mathcal{D}_{out,en}, \mathcal{D}_{nat}\}$ , where  $\mathcal{D}_{nat}$  is collected means that not everyone would encrypt

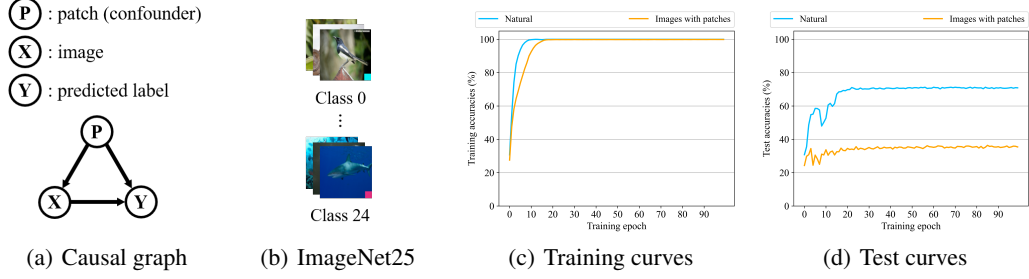


Figure 2: Introducing confounders in ImageNet25 by class-wise patches.

their data before publishing. Then the trainer can label the collected examples  $x$  with classes  $t$  and train the model  $h$  with cross-entropy loss  $\ell$ , as

$$\mathbb{E}_{x \sim \mathcal{P}_{data}} \ell(h(x), t), \quad (1)$$

where  $\mathcal{P}_{data}$  represents the distribution of the training set. Note that data encryptors cannot predict the information of model training in advance (*e.g.*, model backbone, data augmentation), which poses a challenge to the encryption method.

Finally, we measure the effectiveness of the unlearnable example by evaluating the accuracy of model  $h$  on the standard test set  $\mathcal{D}_{test}$ . Intuitively, low test accuracy indicates that the model cannot learn exploitable knowledge from the encrypted dataset.

## 4 Methodology

In this section, we first demonstrate how the native confounder (*i.e.*, background) in the image data affects the performance of a classification model. Inspired by this phenomenon, we introduce a general framework for image data encryption with the causal confounder. Then we instantiate this framework as ConfounderGAN.

### 4.1 Motivation

We observe that the background in some datasets may play the role of the confounder in model learning, thus reducing model performance. Specifically, the image classification task can be modeled as a causal graph. The input image is the cause  $X$ , and the output prediction is the effect  $Y$ . The training process can be regarded as the process of using the ground truth information to regress relationships from images to predictions  $X \rightarrow Y$ . Ideally, if the model can properly learn these true causal relationships, the classification accuracy will be optimal. However, current data-driven deep learning techniques are only good at learning correlations rather than causality, thus the co-occurrence frequency of object and background may influence the model learning *e.g.*, if the dog is always on the grass in the training set, the model may use grass as a key feature of the class dog instead of the dog itself. In other words, the confounder background  $B$  (*i.e.*, grass) constructs a spurious correlation between images and predictions  $X \leftarrow B \rightarrow Y$  so that a biased model is learned. Nevertheless, we also need to be aware that native confounders (*e.g.*, background) in natural datasets do not play a dominant role in training, as models trained on this dataset can still achieve acceptable performance.

### 4.2 Confounder-based encryption framework

Inspired by the above observations, if we can deliberately introduce a confounder  $C$  that is closely related to image  $X$  and label  $Y$  (*i.e.*,  $X \leftarrow C \rightarrow Y$ ), the trained model would hardly learn the correct relationship  $X \rightarrow Y$  from this dataset. We believe this is a general data encryption framework and there are many possible ways to implement it. For example, one straightforward approach is to add class-wise patches (CWP) to the training set. That is, the images of one class add the same patch, while the patches corresponding to each class are different. As shown in Figure 2(a), since the patch is added to the image,  $P \rightarrow X$  is constructed. Meanwhile, the patch of each image is related to the image's class, so this builds the path  $P \rightarrow Y$ . To verify this idea, we select the first 25 classes



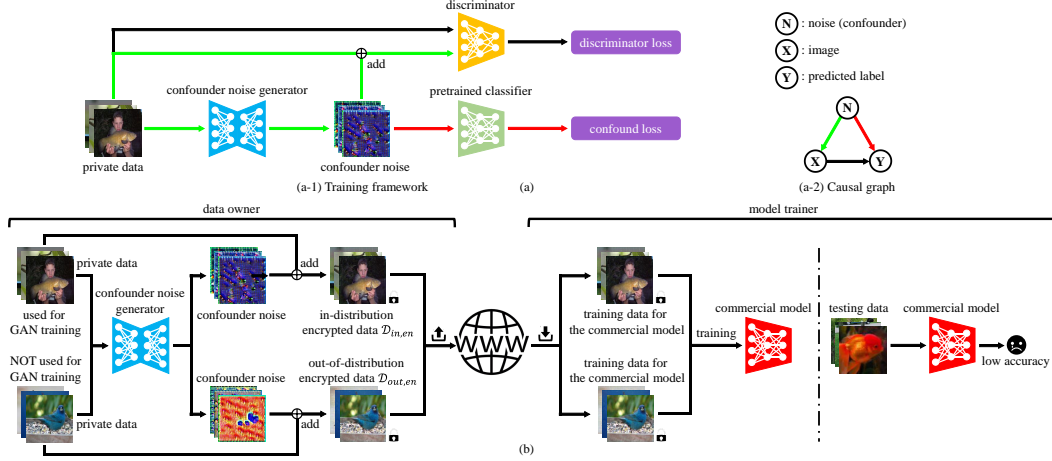


Figure 3: Pipeline of ConfounderGAN: (a) Training pipeline. (b) Evaluation pipeline.

from ImageNet to establish a tiny dataset ImageNet25 for experiments. As illustrated in Figure 2(b), each  $224 \times 224$  image in the training set adds a  $36 \times 36$  patch by class in the lower right corner. More experimental details are elaborated in Appendix G.2. Figure 2(c) and Figure 2(d) shows the training and test accuracy curves during model training, where the final test accuracies on the natural ImageNet25 and the modified ImageNet25 are 70.9% and 35.4%, respectively (Figure 2(d)). This demonstrates that such a simple confounder-based method suppresses the learnable knowledge in the dataset to some extent.

Unfortunately, the patch is too conspicuous in the image, affecting its natural use. A natural idea is to replace class-wise patches with imperceptible class-wise noises (CWN). However, this alternative can be circumvented by early stopping [12], *i.e.*, the model trainer can train a high-accuracy model on this noise-added dataset by early stopping. Meanwhile, both CWP and CWN have two important drawbacks: (1) The patch or the noise is predefined and not correlated with the image, so the relationship between the patch/noise (confounder) and image  $X$  is not strong enough. (2) These methods are limited to in-distribution data encryption and cannot be applied to out-of-distribution data encryption. Hence, how to reasonably introduce a confounder into the training data to overcome the above drawbacks needs to be further explored.

### 4.3 ConfounderGAN: Confounder generation method based on GAN

In order to develop an effective encryption algorithm that can cover various practical scenarios, we utilize adversarial generative networks (GAN) [9] to instantiate the above framework as ConfounderGAN. Our goal is to train a generator whose output confounder noise  $N$  satisfies the causal relationship shown in Figure 3(a-2). Figure 3(a-1) illustrates our overall training pipeline, which mainly consists of three parts: a generator  $G_\theta$  with learnable parameters  $\theta$ , a discriminator  $D_\phi$  with learnable parameters  $\phi$ , and a pretrained classifier  $f_\omega$  with fixed parameters  $\omega$ . The generator  $G_\theta$  takes the private image  $x$  as its input and generates a noise  $G_\theta(x)$ . The encrypted image  $x + G_\theta(x)$  is obtained by combining the original image and noise, as highlighted in green in Figure 3(a-1). We emphasize that this noise as a confounder is better than the predefined class-wise patches and class-wise noises, because its generation relies on the original image, so that the two variables on path  $N \rightarrow X$  have a very strong correlation (Figure 3(a-2)). Then  $x + G_\theta(x)$  will be sent to the discriminator  $D_\phi$ , which is used to distinguish the generated data and the original data  $x$ . The training loss of the discriminator  $D_\phi$  is

$$\mathcal{L}_\phi^{dis}(x) = \mathbb{E}_{x \sim \mathcal{P}_{data}} \log D_\phi(x) + \mathbb{E}_{x \sim \mathcal{P}_{data}} \log(1 - D_\phi(x + G_\theta(x))), \quad (2)$$

where  $\mathcal{P}_{data}$  represents the distribution of the original data. It can be found that the discriminator  $D_\phi$  is a binary classifier that encourages the generated noise to be imperceptible.

Meanwhile, in order to ensure that the generated noise has the confounder property, the relationship  $N \rightarrow Y$  in Figure 3(a-2) needs to be constructed. As highlighted in red in Figure 3(a-1), we achieve

---

**Algorithm 1:** Minibatch training of ConfounderGAN

---

**Input:** a generator  $G_\theta$  with learnable parameters  $\theta$ , a discriminator  $D_\phi$  with learnable parameters  $\phi$ , a pretrained classifier  $f_\omega$  with fixed parameters  $\omega$ , the training epoch is  $M$ , the loss weight factor is  $\alpha$ .

```
1 for  $m = 1, \dots, M$  do
2   Sample minibatch of  $B$  examples  $\{x^{(1)}, \dots, x^{(B)}\}$  with labels  $\{t^{(1)}, \dots, t^{(B)}\}$  from data
   distribution  $\mathcal{P}_{data}$ 
3   Update the discriminator  $D_\phi$  by ascending its gradient:  $\nabla_\phi \frac{1}{m} \sum_{b=1}^B \mathcal{L}_\phi^{dis}(x^{(b)})$ 
4   Update the generator  $G_\theta$  by descending its gradient:
    $\nabla_\theta \frac{1}{m} \sum_{b=1}^B \mathcal{L}_\theta^{confounder}(x^{(b)}, t^{(b)}) + \alpha \mathcal{L}_\theta^{hinge}(x^{(b)})$ 
```

---

this by classifying noise into the ground truth class  $t$  of the original image. Thus training loss of the confounder noise generator  $G_\theta$  is

$$\mathcal{L}_\theta^{confounder}(x, t) = \mathbb{E}_{x \sim \mathcal{P}_{data}} \ell(f_\omega(G_\theta(x)), t), \quad (3)$$

where  $\ell$  denotes the cross-entropy loss commonly used in classification tasks. Note that  $\ell(f_\omega(G_\theta(x)), t)$  in Equation (3) cannot be replaced with  $\ell(f_\omega(x + G_\theta(x)), t)$ , since  $f_\omega(x)$  usually has a high classification accuracy for the original image  $x$ . This means that the loss  $\ell(f_\omega(x), t)$  is low enough, then  $\ell(f_\omega(x + G_\theta(x)), t)$  can be minimized as long as  $G_\theta(x) = 0$ .

To bound the magnitude of the noise and stabilize the GAN’s training [13], we add a soft hinge loss on the  $L_2$  norm as

$$\mathcal{L}_\theta^{hinge}(x) = \mathbb{E}_{x \sim \mathcal{P}_{data}} \max(0, \|G_\theta(x)\|_2 - c), \quad (4)$$

where  $c$  denotes a user-specified bound. Finally, we train the generator  $G_\theta$  and discriminator  $D_\phi$  by solving a max-min game, as

$$\arg \min_{G_\theta} \max_{D_\phi} \mathcal{L}_\phi^{dis}(x) + \mathcal{L}_\theta^{confounder}(x, t) + \alpha \mathcal{L}_\theta^{hinge}(x), \quad (5)$$

where  $\alpha$  controls the weight of  $\mathcal{L}_\theta^{confounder}(x, t)$  and  $\mathcal{L}_\theta^{hinge}(x)$  during generator training. See Algorithm 1 for the pseudo-code of ConfounderGAN.

Once  $G_\theta$  is trained, as illustrated in Figure 3(b), the data owner only needs to input the image into the generator for one forward propagation to achieve the data encryption. If private data is used to train the generator, the processed data is called in-distribution encryption data. Conversely, if private data is NOT used to train the generator, the processed data is called out-of-distribution encryption data. The latter setting is especially useful when the user has some new unlabeled data to encrypt, as it does not need extra training. After this private data is encrypted, the data owner can upload it to the World Wide Web. When the model trainer downloads these images, he/she cannot exploit useful knowledge from these processed images, thus protecting the data privacy of the data owner.

## 5 Experiments

In this section, we first introduce our experimental setup. Then we demonstrate the effectiveness of our proposed method in creating unlearnable examples under in-distribution and out-of-distribution data encryption settings. Next, we conduct a series of transferability and stability of our confounder noise to further illustrate the effectiveness and superiority of our method. Finally, we show some visualizations to better understand our confounder noise.

### 5.1 Experimental setup

We select three natural object datasets and three medical datasets for algorithm evaluation, including SVHN [22], CIFAR10 [16], ImageNet25 [5], BloodMNIST [45], Keratitis and ISIC [1]. See Appendix F for more details on these datasets. We mainly focus on sample-wise noise since it can be applied to various scenarios (e.g., encrypting unlabeled out-of-distribution data). The proposed method is compared with the error-minimizing noise (EMN) [12], which is the strongest baseline for

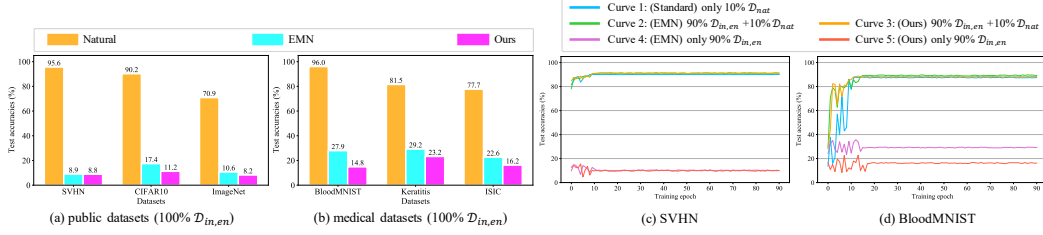


Figure 4: (a)~(b) Test accuracies (%) of the model trained on 100% in-distribution encryption data  $D_{in,en}$  with ResNet18. (c)~(d) Test accuracy curves on SVHN and BloodMNIST

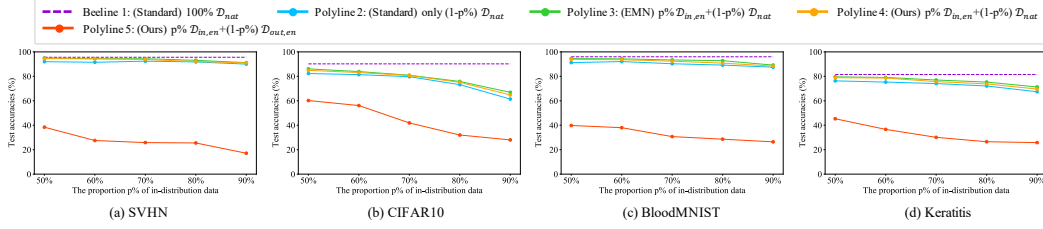


Figure 5: (a)~(d) Effectiveness under different combinations of training data on various datasets with ResNet18 model: lower test accuracy indicates better effectiveness.

data privacy protection. We employ ResNet18 [10] as the source model or pretrained classifier for generating noise, and train ResNet18 on the unlearnable training sets. Referring to Huang et al. [12], the maximum perturbation is set to 8/255 in SVHN and CIFAR10, and 16/255 in other datasets, thus ensuring it is imperceptible to human observers. These settings are fixed for all experiments, unless otherwise explicitly stated. See Appendix G for more experimental details.

## 5.2 Effectiveness of ConfounderGAN

### 5.2.1 In-distribution data encryption

We first examine an extreme case, *if all data collected by the model trainer is in-distribution encryption data (i.e.,  $D_{tr} = 100\% D_{in,en}$ ), how does the model trained on this data perform?* The results are illustrated in Figure 4(a) and Figure 4(b), where ‘natural’ represents the original image. The corresponding test accuracies of EMN and our method demonstrate that the learnable knowledge of images is effectively suppressed. More importantly, all datasets processed by our method have the lowest accuracy, which proves the superiority of our method in data privacy protection.

However, in most situations, not all the training data collected by the model trainer are unlearnable examples. For example, only a certain number of web users have decided to use protection techniques but not all users. Thus, one question is naturally raised: *If the trainer uses  $p\%$  in-distribution encryption data  $D_{in,en}$  and  $(1 - p\%)$  natural data  $D_{nat}$  for model training, can these encryption data  $D_{in,en}$  still maintain the unlearnable property in this mixed dataset?* For validation, we train the model on only the natural proportion  $(1 - p\%) D_{nat}$  for comparison. The results are shown in Figure 5, where the X-axis represents the proportion  $p\%$  of  $D_{in,en}$  to the original total dataset and the Y-axis represents the classification accuracy on the same test set  $D_{test}$ . A quick glance at Polyline 3 and Polyline 4 tells us that the effectiveness of both EMN and our method drops quickly when the data are not made 100% unlearnable, because their accuracy is close to Beeline 1 (i.e., 100% natural dataset). This means that the encryption effect can be approximately ignored even when the noise is applied to 50% of the data. However, we can also observe that Polyline 2 is close to Polyline 3 and Polyline 4, which may indicate that the high test accuracy in Polyline 3 and Polyline 4 is caused by  $(1 - p\%)$  natural data  $D_{nat}$ .

To illustrate this, we take  $p = 90\%$  in SVHN and BloodMNIST as examples and plot their test accuracy curves during training as shown in Figure 4(c) and Figure 4(d). We additionally add Curve 4 and Curve 5 that only use 90% in-distribution encryption data  $D_{in,en}$  for model training. The result of these two curves demonstrates that 90%  $D_{in,en}$  is still unlearnable and the test accuracy curve of our method is significantly lower than that of EMN on BloodMNIST, which is consistent with the

Dataset	SVHN			CIFAR10			ImageNet25		
	Natural	EMN	Ours	Natural	EMN	Ours	Natural	EMN	Ours
VGG11	95.0	32.6	<b>25.4</b>	86.2	19.1	<b>16.9</b>	62.6	34.0	<b>26.5</b>
ResNet50	95.9	10.6	<b>10.1</b>	91.5	17.9	<b>11.3</b>	73.6	12.3	<b>8.4</b>
DenseNet121	96.3	10.9	<b>8.9</b>	92.6	18.6	<b>13.4</b>	80.0	11.3	<b>9.5</b>

Dataset	BloodMNIST			Keratitis			ISIC		
	Natural	EMN	Ours	Natural	EMN	Ours	Natural	EMN	Ours
VGG11	96.3	35.4	<b>29.7</b>	79.8	55.4	<b>35.6</b>	72.6	45.6	<b>18.7</b>
ResNet50	95.7	41.7	<b>31.4</b>	80.2	34.4	<b>26.6</b>	75.3	24.3	<b>18.0</b>
DenseNet121	97.0	35.4	<b>27.5</b>	88.4	30.7	<b>27.0</b>	81.9	26.7	<b>22.7</b>

Table 1: Transferability results: the unlearnable noise is customized for ResNet18, while the evaluation is performed on VGG11, ResNet50, DenseNet121.

Method	No augmentation	RHF	RC	RHF+RC
EMN	17.4	17.9	18.0	18.3
Ours	<b>11.2</b>	<b>11.9</b>	<b>14.8</b>	<b>14.9</b>

Method	CutOut	MixUp	CutMix	FA
EMN	18.2	25.7	18.6	<b>38.4</b>
Ours	<b>15.0</b>	<b>19.3</b>	<b>13.6</b>	39.3

Table 2: Test accuracies (%) of the ResNet18 model trained on unlearnable CIFAR-10 with various data augmentation.

result of BloodMNIST in Figure 4(b) (100%  $\mathcal{D}_{in,en}$ ). Meanwhile, Curve 1, Curve 2 and Curve 3 are almost the same, showing that the exploitable knowledge in Curve 2 and Curve 3 mainly comes from 10% natural data. Therefore, we conclude that both images encrypted by our method or EMN remain unlearnable property even as part of the dataset, and our method maintains its superiority to some extent. In addition, we also provide training gradient analysis on our encrypted images in the Appendix A to better understand the effectiveness of our method.

### 5.2.2 Out-of-distribution data encryption

In real-world scenarios, people sometimes want to quickly encrypt their instant photos with little computing resources. For example, a person takes a photo with a cell phone and plans to upload it to social media immediately. EMN is hard to deploy in this lightweight computing setting, as it needs multiple bi-level gradient optimizations to generate an effective noise. In contrast, in our ConfounderGAN, once the confounder noise generator  $G_\theta$  is trained, it only needs to input any image into  $G_\theta$  for one forward-propagation to achieve encryption, and no label information is required, which is ideal for the above practical scenario. However, since the generator has not seen these newly captured images during training, the effectiveness of the generated noise on these out-of-distribution images is unknown. Therefore, we try to explore the following question: *If the trainer uses  $p\%$  in-distribution encryption data  $\mathcal{D}_{in,en}$  and  $(1 - p\%)$  out-of-distribution encryption data  $\mathcal{D}_{out,en}$  for model training, can these out-of-distribution encryption data  $\mathcal{D}_{out,en}$  effectively suppress the learnable information?* For brevity, we plot the experimental results to Polyline 5 in Figure 5. The generator for each point in Polyline 4 and Polyline 5 is trained with the same  $p\%$  data, and performs in-distribution encryption on these data after training. The main difference between Polyline 4 and Polyline 5 is that the former does not encrypt the remaining  $(1 - p\%)$  natural data, while the latter performs out-of-distribution encryption for these remaining data. It can find that the test accuracies of Polyline 5 are obviously lower than those of Polyline 4, which demonstrates that the out-of-distribution data encrypted by our method has significantly less learnable knowledge than the natural data  $\mathcal{D}_{nat}$ , thus proving the effectiveness of our method for out-of-distribution personal data. See Appendix E for more experiments.

## 5.3 A Series of Analytical Experiments about ConfounderGAN

For simplicity, the analytical experiments in this subsection are all conducted under the 100% in-distribution encryption setting (*i.e.*, 100%  $\mathcal{D}_{in,en}$ ), unless otherwise stated.

### 5.3.1 Transferability analysis

Both EMN and our ConfounderGAN rely on a pretrained classifier  $f$  to generate effective unlearnable noise. Specifically, EMN uses this classifier as a source model to compute the gradient of error-



Figure 6: Visualization: Orig. represents the original image, Enc. represents the encrypted image.

minimizing noise, and our ConfounderGAN needs this classifier to learn the correlation between the confounder noise and the label. Therefore, it can be considered that unlearnable noise is customized for this classifier  $f$ . If the pretrained classifier  $f$  used by the data owner and the commercial model  $h$  trained by the unauthorized company share the same backbone, the protection performance should be optimal and the above experiments follow this setting (*i.e.*, both are ResNet18). However, in practical scenarios, the data owner cannot predict which model  $h$  the trainer will choose as the backbone. A natural concern is raised: *If the architecture of classifier  $f$  and model  $h$  are different, can the unlearnable property of the noise trained on classifier  $f$  be transferable to the model  $h$ ?* Table 1 shows the results of the transferability under in-distribution encryption setting (*i.e.*, 100%  $\mathcal{D}_{in,en}$ ), where the classifier  $f$  employs ResNet18 and the model  $h$  selects VGG11 [34], ResNet50 and DenseNet121 [11]. The results show our method outperforms EMN on all datasets and evaluated models, especially for VGG11, indicating that our confounder noise is more practical and effective.

### 5.3.2 Stability analysis

Model trainers are likely to use some data augmentation techniques to improve their model performance during the training phase, so a question is introduced: *Can noise still work well with different data augmentations?* To answer this question, we select 7 commonly used and advanced data augmentation techniques for evaluation on CIFAR10: Random Horizontal Flip (RHF), Random Crop (RC), Combination of Horizontal Flip and Crop (RHF+RC), CutOut [7], MixUp [47], CutMix [46], Fast Autoaugment (FA) [19]. See Appendix G.6 for detailed experimental setup. The results are shown in Table 2. It can be observed that the noise still maintains high effectiveness in most settings. Meanwhile, the test accuracies of our method are also lower than those of EMN in all cases, which further proves that our method is better than EMN. In addition, we also investigate the stability of ConfounderGAN under early stopping and adaptive setting. See Appendix C and Appendix D for more details.

## 5.4 Visualizations

As shown in Figure 6, we randomly select two images from the ImageNet25 for visualization. Since noises are all limited to a small range, all noises are scaled to the interval  $[0, 255]$  according to their maximum and minimum values. We can observe that the noises of EMN are small disordered dots in most cases, while the noises of our method show some high-level representations. *e.g.*, feather-like textures can be observed. These high-level representations may lead to the better transferability of our method (as mentioned in Section 5.3.1), since different backbones may share some common representations. See Appendix B for more visualizations.

## 6 Conclusion

We focus on the image data encryption task, its goal is to use small and invisible noise to prevent personal data from being freely exploited by deep neural networks. By leveraging confounder property, we propose a confounder-based encryption framework for image data. *i.e.*, introduce a confounder that is strongly correlated with both images and labels in the dataset, so that the model trained on this dataset can only learn the spurious correlations between images and labels. Based on this framework, we develop confounderGAN, a novel image data encryption method that covers various practical scenarios. Empirically, we demonstrate that our method outperforms the state-of-the-art algorithm in the in-distribution data encryption and can be effectively applied to out-of-distribution data encryption. Moreover, we also verify that the transferability and robustness of our confounder noise. We believe this paper provides new insight into data privacy protection and could have a broad impact on both the public and the deep learning community.

## 7 Acknowledgements

This work was supported in part by National Natural Science Foundation of China (No. 62006207, No. 62037001), the Starry Night Science Fund of Zhejiang University Shanghai Institute for Advanced Study (SN-ZJU-SIAS-0010), Key Laboratory for Corneal Diseases Research of Zhejiang Province, Project by Shanghai AI Laboratory (P22KS00111), Program of Zhejiang Province Science and Technology (2022C01044), the Fundamental Research Funds for the Central Universities (226-2022-00142, 226-2022-00051), Zhejiang Province Natural Science Foundation (No. LQ21F020020) and National Natural Science Foundation of China (Grant No. U20A20387).

## References

- [1] Matt Berseth. Isic 2017-skin lesion analysis towards melanoma detection. *arXiv preprint arXiv:1703.00523*, 2017.
- [2] Battista Biggio, Blaine Nelson, and Pavel Laskov. Poisoning attacks against support vector machines. *arXiv preprint arXiv:1206.6389*, 2012.
- [3] Abeba Birhane and Vinay Uday Prabhu. Large image datasets: A pyrrhic win for computer vision? In *WACV*, 2021.
- [4] Xinyun Chen, Chang Liu, Bo Li, Kimberly Lu, and Dawn Song. Targeted backdoor attacks on deep learning systems using data poisoning. *arXiv preprint arXiv:1712.05526*, 2017.
- [5] Jia Deng, Wei Dong, Richard Socher, Li-Jia Li, Kai Li, and Li Fei-Fei. Imagenet: A large-scale hierarchical image database. In *CVPR*, 2009.
- [6] Jacob Devlin, Ming-Wei Chang, Kenton Lee, and Kristina Toutanova. Bert: Pre-training of deep bidirectional transformers for language understanding. In *NAACL-HLT*, 2019.
- [7] Terrance DeVries and Graham W Taylor. Improved regularization of convolutional neural networks with cutout. *arXiv preprint arXiv:1708.04552*, 2017.
- [8] Ji Feng, Qi-Zhi Cai, and Zhi-Hua Zhou. Learning to confuse: generating training time adversarial data with auto-encoder. In *NeurIPS*, 2019.
- [9] Ian Goodfellow, Jean Pouget-Abadie, Mehdi Mirza, Bing Xu, David Warde-Farley, Sherjil Ozair, Aaron Courville, and Yoshua Bengio. Generative adversarial nets. In *NeurIPS*, 2014.
- [10] Kaiming He, Xiangyu Zhang, Shaoqing Ren, and Jian Sun. Deep residual learning for image recognition. In *CVPR*, 2016.
- [11] Gao Huang, Zhuang Liu, Laurens Van Der Maaten, and Kilian Q Weinberger. Densely connected convolutional networks. In *CVPR*, 2017.
- [12] Hanxun Huang, Xingjun Ma, Sarah Monazam Erfani, James Bailey, and Yisen Wang. Unlearnable examples: Making personal data unexploitable. In *ICLR*, 2021.
- [13] Phillip Isola, Jun-Yan Zhu, Tinghui Zhou, and Alexei A Efros. Image-to-image translation with conditional adversarial networks. In *CVPR*, 2017.
- [14] Xiaojun Jia, Xingxing Wei, Xiaochun Cao, and Xiaoguang Han. Adv-watermark: A novel watermark perturbation for adversarial examples. In *MM*, 2020.
- [15] Jayendra Kantipudi, Shiv Ram Dubey, and Soumendu Chakraborty. Color channel perturbation attacks for fooling convolutional neural networks and a defense against such attacks. *TIP*, 2020.
- [16] Alex Krizhevsky et al. Learning multiple layers of features from tiny images. *Citeseer*, 2009.
- [17] Kun Kuang, Lian Li, Zhi Geng, Lei Xu, Kun Zhang, Beishui Liao, Huaxin Huang, Peng Ding, Wang Miao, and Zhichao Jiang. Causal inference. *Engineering*, 2020.
- [18] Jiahui Li, Kun Kuang, Baoxiang Wang, Furui Liu, Long Chen, Changjie Fan, Fei Wu, and Jun Xiao. Deconfounded value decomposition for multi-agent reinforcement learning. In *ICML*, 2022.

- [19] Sungbin Lim, Ildoo Kim, Taesup Kim, Chiheon Kim, and Sungwoong Kim. Fast autoaugment. In *NeurIPS*, volume 32, 2019.
- [20] Yunfei Liu, Xingjun Ma, James Bailey, and Feng Lu. Reflection backdoor: A natural backdoor attack on deep neural networks. In *ECCV*, 2020.
- [21] Luis Muñoz-González, Battista Biggio, and Ambra Demontis. Towards poisoning of deep learning algorithms with back-gradient optimization. In *AISec*, 2017.
- [22] Yuval Netzer, Tao Wang, Adam Coates, and Alessandro Bissacco. Reading digits in natural images with unsupervised feature learning. 2011.
- [23] Nature News. Google health-data scandal spooks researchers. In *Nature News*, 2019.
- [24] Judea Pearl. *Causality*. Cambridge university press, 2009.
- [25] Fabien Petitcolas. La cryptographie militaire. *J. des Sci. Militaires*, 1883.
- [26] NhatHai Phan, Yue Wang, and Xintao Wu. Differential privacy preservation for deep auto-encoders: an application of human behavior prediction. In *AAAI*, 2016.
- [27] NhatHai Phan, Xintao Wu, Han Hu, and Dejing Dou. Adaptive laplace mechanism: Differential privacy preservation in deep learning. In *ICDM*, 2017.
- [28] Evani Radiya-Dixit and Florian Tramèr. Data poisoning won’t save you from facial recognition. *arXiv preprint arXiv:2106.14851*, 2021.
- [29] Ali Shafahi, W Ronny Huang, Mahyar Najibi, and Octavian Suciu. Poison frogs! targeted clean-label poisoning attacks on neural networks. In *NeurIPS*, 2018.
- [30] Shawn Shan, Emily Wenger, Jiayun Zhang, Huiying Li, Haitao Zheng, and Ben Y Zhao. Fawkes: Protecting privacy against unauthorized deep learning models. In *USENIX Security*, 2020.
- [31] Zheyang Shen, Peng Cui, Kun Kuang, Bo Li, and Peixuan Chen. Causally regularized learning with agnostic data selection bias. In *MM*, 2018.
- [32] Reza Shokri and Vitaly Shmatikov. Privacy-preserving deep learning. In *SIGSAC*, 2015.
- [33] Reza Shokri, Marco Stronati, Congzheng Song, and Vitaly Shmatikov. Membership inference attacks against machine learning models. In *SP*, 2017.
- [34] Karen Simonyan and Andrew Zisserman. Very deep convolutional networks for large-scale image recognition. *arXiv preprint arXiv:1409.1556*, 2014.
- [35] New York Times. The secretive company that might end privacy as we know it. In *New York Times*, 2020.
- [36] Tan Wang, Jianqiang Huang, Hanwang Zhang, and Qianru Sun. Visual commonsense r-cnn. In *CVPR*, 2020.
- [37] Wikipedia. Project nightingale. In *Wikipedia*, 2019.
- [38] Wikipedia. Electronic communications privacy act. In *Wikipedia*, 2021.
- [39] Wikipedia. General data protection regulation. In *Wikipedia*, 2021.
- [40] Wikipedia. Health insurance portability and accountability act. In *Wikipedia*, 2021.
- [41] Wikipedia. Information privacy law. In *Wikipedia*, 2021.
- [42] Anpeng Wu, Kun Kuang, Bo Li, and Fei Wu. Instrumental variable regression with confounder balancing. In *ICML*, 2022.
- [43] Anpeng Wu, Junkun Yuan, Kun Kuang, Bo Li, Runze Wu, Qiang Zhu, Yue Ting Zhuang, and Fei Wu. Learning decomposed representations for treatment effect estimation. *TKDE*, 2022.

- [44] Chaofei Yang, Qing Wu, Hai Li, and Yiran Chen. Generative poisoning attack method against neural networks. *arXiv preprint arXiv:1703.01340*, 2017.
- [45] Jiancheng Yang, Rui Shi, Donglai Wei, Zequan Liu, Lin Zhao, and Bilian Ke. Medmnist v2: A large-scale lightweight benchmark for 2d and 3d biomedical image classification. *arXiv preprint arXiv:2110.14795*, 2021.
- [46] Sangdoo Yun, Dongyoon Han, and Seong Joon Oh. Cutmix: Regularization strategy to train strong classifiers with localizable features. In *ICCV*, 2019.
- [47] Hongyi Zhang, Moustapha Cisse, Yann N Dauphin, and David Lopez-Paz. mixup: Beyond empirical risk minimization. *arXiv preprint arXiv:1710.09412*, 2017.
- [48] Kai Zhang, Wangmeng Zuo, Yunjin Chen, Deyu Meng, and Lei Zhang. Beyond a gaussian denoiser: Residual learning of deep cnn for image denoising. *TIP*, 2017.



## A Gradient analysis

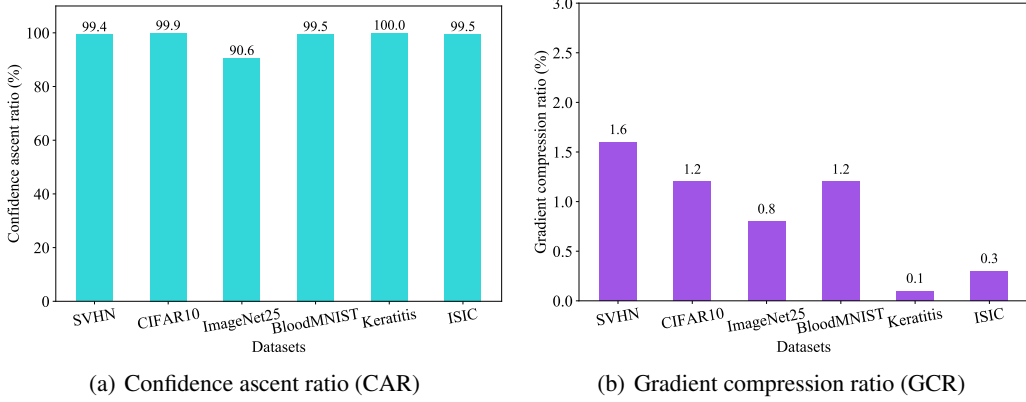


Figure 7: Confidence ascent ratio (CAR) and Gradient compression ratio (GCR) on various datasets.

To better understand why our generated confounder noise can make the data unlearnable, we can also gain some insights according to optimization gradient. Empirically, if one image provides a large gradient in a backpropagation, this image has a lot of learnable knowledge, and vice versa. Thus a natural question is: *How do the confidence and optimization gradients produced by our encrypted dataset change relative to those of the original dataset during model training?* We propose two statistical metrics for validation: Confidence Ascent Ratio (CAR) and Gradient Compression Ratio (GCR). Specifically, suppose that the training model is  $h$  with the parameters of the last layer (classifier)  $W$ , the number of images in the training set  $\mathcal{D}_{tr}$  is  $n$ . The confidence of the original image  $x$  corresponding to ground truth class  $t$  is  $h(x)_t$ , and this confidence of the encrypted image is  $x + G_\theta(x)$  is  $h(x + G_\theta(x))_t$ , then CAR is defined as

$$\text{CAR} = \frac{\sum_{x \in \mathcal{D}_{tr}} \mathbb{1}((h(x + G_\theta(x)))_t - h(x)_t) > 0)}{n}, \quad (6)$$

where  $\mathbb{1}(\cdot)$  is a indicator function. GCR is defined as

$$\text{GCR} = \frac{\sum_{x \in \mathcal{D}_{tr}} (\|\nabla_W \ell(x + G_\theta(x), t)\|_2 / \|\nabla_W \ell(x, t)\|_2)}{n}. \quad (7)$$

where  $\|\cdot\|_2$  represents the  $L_2$  norm,  $\nabla_W \ell(\cdot)$  represents the gradient of the given input w.r.t. the classifier.

Figure 7 demonstrates CAR and GCR in all datasets, where the checkpoint of model  $h$  is randomly selected during the training phase. From the result of Figure 7(a), we can find that CAR exceeds 90% in all datasets and even reaches 100% in Keratitits. This means that most images can be correctly classified by the model  $h$  after adding our confounder noise, so that the model ‘thinks’ that these encrypted images have nothing to learn. This phenomenon can be understood because the confounder noise and the label have a strong correlation in ConfounderGAN. Further, we can observe that GCR is less than 2% for all datasets in Figure 7(b). That is, the backpropagation gradient provided by the encrypted image  $x + G_\theta(x)$  to the deep neural network is less than 2% of that provided by the original image  $x$ , which fully shows the exploitable knowledge in  $x + G_\theta(x)$  is greatly suppressed compared to  $x$ .

## B Visualization

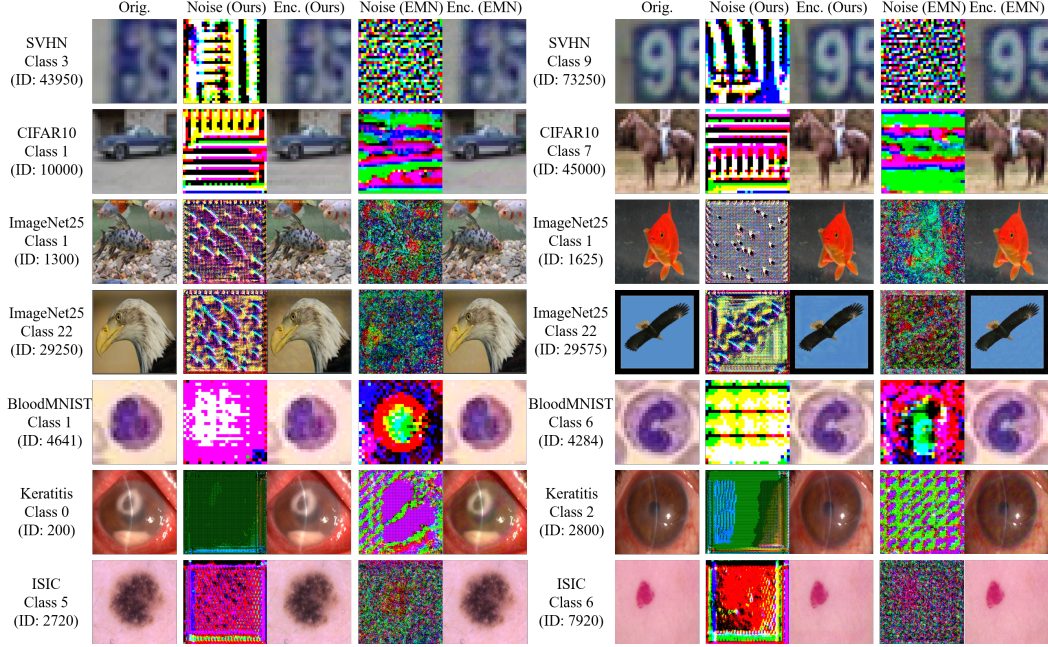


Figure 8: Visualization: Orig. represents the original image, Enc. represents the encrypted image.

## C Stability analysis about early stopping

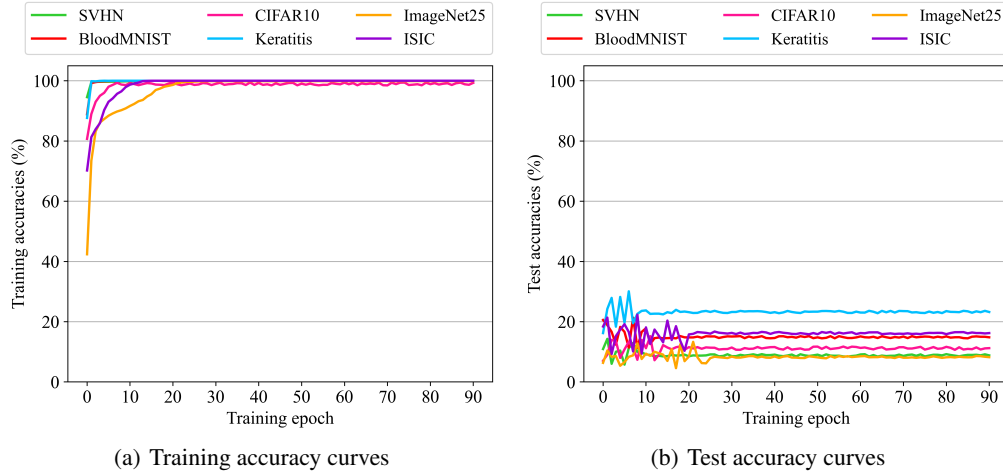


Figure 9: Training and test accuracy curves on different datasets during model training.

Huang et al. [12] find that if the model is trained on the dataset with predefined class-wise noises, it can achieve satisfactory test accuracy in the early stage of training. This means that the model trainer can use early stopping to circumvent the protection of predefined class-wise noises. Then they prove that their proposed EMN does not suffer from the above phenomenon. We are also curious: *Is the noise generated by our ConfounderGAN effective for the entire epoch of training?* Figure 9 shows the accuracy curves of our method during the training epoch. It reveals that the model always has low test accuracy at all stages of training, so the early stopping trick cannot circumvent our confounder noise.

## D Stability analysis about adaptive setting

In this section, we first conduct the experiment to investigate the effectiveness of our method under the adaptive setting proposed by [28]. Then we give a detailed discussion about this setting.

To better understand this adaptive setting, we first illustrate the assumption on the data owner’s capability and the model trainer’s capability under this setting:

**Assumption on data owner’s capability:** A data owner processes some natural images  $\mathcal{D}_{nat}$  into encrypted images  $\mathcal{D}_{en}$  via ConfounderGAN and uploads them to social media.

**Assumption on model trainer’s capability:** A model trainer knows that these images  $\mathcal{D}_{en}$  have been processed by ConfounderGAN and can directly access the generator of ConfounderGAN. The model trainer wishes to train a denoiser against the noise generated by the ConfounderGAN. However, the trainer cannot obtain the original images  $\mathcal{D}_{nat}$  corresponding to the encrypted images  $\mathcal{D}_{en}$ , otherwise he/she can directly use these original images  $\mathcal{D}_{nat}$  to train the model. Therefore, in order to denoise the encrypted images  $\mathcal{D}_{en}$ , the model trainer needs to do the following steps: 1) collect additional natural images  $\mathcal{D}'_{nat}$ . 2) feed the surrogate images  $\mathcal{D}'_{nat}$  into the generator of ConfounderGAN to build the encrypted images  $\mathcal{D}'_{en}$ . 3) use  $\mathcal{D}'_{nat}$  and  $\mathcal{D}'_{en}$  to train a denoiser. 4) remove the noise of the encrypted images  $\mathcal{D}_{en}$  by the trained denoiser.

We conduct the experiment on CIFAR10 to investigate whether the adaptive denoiser can completely remove the effect of the encrypted noises. In practice, we divide the training set of CIFAR10 into two equally as  $\mathcal{D}_{nat}$  and  $\mathcal{D}'_{nat}$ , and then use the above steps to obtain the denoised images, where the training of the denoiser follows DnCNN [48]. The experimental results are shown in the table below.

Training dataset	Natural images	Denoised images	Encrypted images
Test accuracy	87.4%	77.9%	11.9%

Table 3: Test accuracies (%) of the model trained on different datasets.

The result shows that although the denoiser can resist our encryption method to a certain extent, the model’s performance can still be compromised by our confounder noises, which shows that our method retains its effectiveness under the adaptive setting.

Meanwhile, for the adaptive setting proposed by Radiya-Dixit et al. [28], we believe there are two important points that need to be clarified.

**1) We believe that this adaptive setting has unbalanced assumptions about the strength of the data owner’s capability and model trainer’s capability, leaving the data owner (or crypto tool designer) on the weaker side.** Specifically, Radiya-Dixit et al. [28] assume that the model trainer has full access to the encryption tool, while the crypto tool designer has no knowledge of the model trainer’s decryption method. For example, in our paper, ConfounderGAN’s designer does not know that the model trainer will use a denoiser to remove encryption noises. However, if we know this information in advance, we might be able to introduce the knowledge of the denoiser into the training process of the ConfounderGAN, making it robust to the denoiser. An intuitive idea is to change the existing training architecture from ‘original image -> generator -> confounder noise -> pretrain classifier’ to ‘original image -> generator -> confounder noise -> **pretrain denoiser** -> pretrain classifier’, so that the confounder property can be preserved even if the generated noises encounter a denoiser in the future. Of course, this solution is very rudimentary. We will explore the optimal solution in future work, thus giving the data owner (or crypto tool designer) an edge in the arms race with the model trainer.

**2) Since data owners usually don’t reveal which encryption tool they use, we believe that the non-adaptive setting may be more practical than the adaptive setting in real-world scenarios.** Specifically, Radiya-Dixit et al. [28] believe that the adaptive setting is practical in the real-world, and they give the following argument: encryption tools are usually publicly accessible applications, thus model trainers can adaptively train a feature extractor that resists these encryption noises. We agree that encryption tools are generally publicly accessible, but disagree that model trainers can adaptively train feature extractors. This is because multiple encryption methods will be proposed in the future. When data owners publish encrypted data, they won’t reveal the encryption tools they use in most scenarios. Thus it is difficult for the model trainers to determine which encryption method should be

used when adaptively training decryption feature extractors. In fact, referring to the community of adversarial examples [14, 15], one encryption method can derive multiple instantiations by modifying the encryption constraints. For example, data owners can replace small pixel-wise perturbation with watermark [14], color channel perturbation [15], *etc.*, according to their preferences. As long as the data owner does not expose the information of the encryption tool, the model trainer cannot decrypt it in an adaptive manner. Based on these analyses, we believe that the non-adaptive setting may be more practical than the adaptive setting in real-world scenarios. Note that this does not mean that the adaptive setting is unnecessary, we realize that it is important to design an encryption tool that strictly satisfies the Kerckhoffs’s principle [25]. In future work, we will further improve ConfounderGAN so that it can work optimally under this principle.

## E Comparing CounfounderGAN with DeepConfuse under out-of-distribution encryption

We notice that DeepConfuse [8] can also be applied to out-of-distribution (OOD) data encryption. Therefore, we compare the effectiveness of this method in the OOD setting with our method. The experiment is conducted on CIFAR10 and the evaluation settings are consistent with Figure 6(b) of the manuscript. The experimental results are as follows:

Method	$p\% \mathcal{D}_{in,en} + (1-p\%) \mathcal{D}_{out,en}$				
	p=50%	p=60%	p=70%	p=80%	p=90%
DeepConfuse	71.3%	61.6%	50.2%	45.8%	36.3%
Ours	60.2%	56.1%	41.9%	32.0%	28.0%

Table 4: Test accuracies (%) under different combinations of training data.

We can find that the dataset processed by our ConfounderGAN can obtain lower test accuracy, indicating that our method outperforms DeepConfuse for out-of-distribution encryption.

## F Datasets

We show some key information about each dataset to better understand our experiments.

**SVHN<sup>2</sup>**. SVHN is a digit dataset, containing numbers 0 to 9. This dataset is collected from house numbers in Google Street View images with low resolution, which consists of 73,257 training images and 26,032 test images in 10 classes. The number of each class in the training and test sets is unbalanced. All images are  $3 \times 32 \times 32$  three-channel color images.

**CIFAR10<sup>3</sup>**. CIFAR10 are labeled subsets of the 80 million tiny images dataset. The latter is automatically downloaded from the Internet through a crawler script, and this unauthorized data collection matches the scenario assumed in this paper. CIFAR10 consists of 50,000 training images and 10,000 test images in 10 classes, classes, with 5,000 and 1,000 images per class. All images are  $3 \times 32 \times 32$  three-channel color images.

**ImageNet25<sup>4</sup>**. ImageNet25 is a subset of the ImageNet dataset (the first 25 classes). The experiments on this dataset are to confirm the effectiveness of the method on high-resolution images. It consists of 32,500 training images and 1,250 test images, with 1,250 and 50 images per class. All images are  $3 \times 224 \times 224$  three-channel color images.

**BloodMNIST<sup>5</sup>**. BloodMNIST is based on a dataset of individual normal cells, captured from individuals without infection, hematologic or oncologic disease. It is organized into 8 classes and consists of 11,959 training images and 3,421 test images. The number of each class in the training and test sets is unbalanced. All images are  $3 \times 28 \times 28$  three-channel color images.

<sup>2</sup><http://ufldl.stanford.edu/housenumbers/>

<sup>3</sup><https://www.cs.toronto.edu/~kriz/cifar.html>

<sup>4</sup><https://www.image-net.org/>

<sup>5</sup><https://medmnist.com/>

**Keratitis.** This dataset is collected at our local hospital to evaluate the effectiveness of the method in real-world scenarios. It consists of 4,047 training images and 581 test images in 4 classes. The number of each class in the training and test sets is unbalanced. All images are  $3 \times 224 \times 224$  three-channel color images.

**ISIC<sup>6</sup>.** ISIC is a high-resolution medical datasets, which is collected from leading international clinical centers. This dataset consists of 8,005 training images and 2,010 test images in 7 classes. The number of each class in the training and test sets is unbalanced. All images are  $3 \times 224 \times 224$  three-channel color images.

## G Experimental setup

### G.1 Hardware

In all experiments, the GPU is NVIDIA GTX 1080Ti and the CPU is Intel(R) Xeon(R) E5-2678 v3 @ 2.50GHz.

### G.2 Experimental setup for toy experiments

In the class-wise patches experiment, we select the first 25 classes from ImageNet to construct a new dataset ImageNet25 for evaluation. In the training set, each  $224 \times 224$  image adds a  $32 \times 32$  patch by class in the lower right corner. Since images of ImageNet are color images, the added patches are also three-channel color images. To simplify, we design the value of each patch by channel. *e.g.*, the patch for Class 0 is represented as (220,0,0), which means that all the pixels of the first channel are 220 and the other channels are all 0. Then we list the patch for all classes: (220,0,0),(230,0,0),(240,0,0),(250,0,0),(0,220,0),(0,230,0),(0,240,0),(0,250,0),(0,0,220),(0,0,230),(0,0,240),(0,0,250),(220,220,0),(230,230,0),(240,240,0),(250,250,0),(220,0,220),(230,0,230),(240,0,240),(250,0,250),(220,0,220),(230,0,230),(240,0,240),(250,0,250),(250,250,250).

We use ResNet18 as the backbone. The hyperparameters for model training are listed as follows: the optimizer is SGD, momentum is 0.9, initial learning rate is 0.025, the learning rate scheduler is cosine scheduler without the restart, training epoch is 90.

### G.3 Experimental setup for ConfounderGAN

ConfounderGAN contains three neural networks: a generator, a discriminator and a pretrained classifier. The generator consists of a 4-layer convolutional neural network and a 4-layer deconvolutional neural network. The discriminator consists of a 4-layer convolutional neural network and a binary classifier. The pretrained classifier is ResNet18. The input and output layers of the generator and pretrained classifier are adjusted according to the image size and class number of each dataset. The classifiers for all datasets are pretrained on their training set, except for ImageNet where the pretrained model is downloaded directly from the Pytorch official website.

The training of ConfounderGAN consists of generator training and discriminator training. The hyperparameters for generator training is listed as follows: the optimizer is SGD, the momentum is 0.9, the initial learning rate is 0.025, the learning rate scheduler is cosine scheduler without the restart, the loss weight factor is 0.001, the training epoch is 200(SVHN,CIFAR10,Keratitis)/5000(ImageNet25)/100(BloodMNIST)/400(ISIC). The training hyperparameters of the discriminator refer to those of the generator, except that the learning rate is set to a constant 0.025.

### G.4 Experimental setup for EMN

EMN requires a source model as a surrogate model to compute the noise gradient. Referring to the original paper, the backbone of this model architecture is ResNet18.

EMN is a two-level optimization method. The inner loop generates noise, and its hyperparameters are as follows: the optimizer is SGD, the learning rate is 0.003, the number of iterations is 20. The outer loop updates the source model with the following hyperparameters: the optimizer is SGD, the

<sup>6</sup><https://challenge2018.isic-archive.com/>

learning rate is 0.003, the number of iterations is 10. The stopping condition for training is that the error of the source model on the training set is 0.01.

### **G.5 Experimental setup for evaluation**

We need to train a model  $h$  on the unlearnable dataset to prove the effectiveness of the encryption algorithm. In our experiments, all datasets share a set of hyperparameters for training model  $h$ : the optimizer is SGD, the momentum is 0.9, the initial learning rate is 0.025, the learning rate scheduler is cosine scheduler without the restart, the training epoch is 90.

### **G.6 Experimental setup for data augmentations**

For RC, we set the padding length to 4 pixels. For CutOut, we set the cutout length to 16 pixels. For MixUp, we apply linear mixup of random pairs of training examples and their labels during the training process. For CutMix, we apply linear mixup on the cutout region. For FA, we use the fixed augmentation policy, which consists of change contrast, brightness, sharpness, rotations and cutout.